Mol Breeding
DOI 10.1007/s11032-014-0162-8

Downregulation of polyphenol oxidase in potato tubers redirects phenylpropanoid metabolism enhancing chlorogenate content and late blight resistance

Briardo Llorente · Mariana G. López · Fernando Carrari · Ramón Asís · Romina D. Di Paola Naranjo · Mirtha M. Flawiá · Guillermo D. Alonso · Fernando Bravo-Almonacid

Received: 29 April 2014 / Accepted: 25 July 2014

Abstract Land plants synthesize phenolic compounds involved in plant defense against invading pathogens through the phenylpropanoid pathway. Although not considered as part of the phenylpropanoid pathway, plant polyphenol oxidases (PPOs) are enzymes that catalyze cresolase and catecholase reactions on several phenolic compounds. Here, transgenic potato (*Solanum tuberosum*) tubers with downregulated *PPO* genes (-PPO) were challenged with the oomycete pathogen *Phytophthora infestans* to investigate the interactions between PPO, phenylpropanoid metabolism, and disease resistance. We found that pathogen invasiveness was reduced in -PPO lines, while microscopic evidences suggested that the mechanism underlying the defense response involved the participation of phenolic compounds. Detailed metabolite-profiling analyses demonstrated that the concentration of metabolites related to the phenylpropanoid pathway and chlorogenate in particular was largely altered in PPO-downregulated tubers. Silencing of PPO caused a shift in metabolism from phenylpropanoid precursors to downstream phenylpropanoid products. The presented results suggest that downregulation of PPO redirects the phenylpropanoid metabolism leading to the accumulation of defensive phenolic compounds in the plant cells, consequently enhancing resistance to the pathogen. These results emphasize the importance of components acting in parallel to canonical metabolic pathway constituents in influencing plant metabolism and reveal new

Electronic supplementary material The online version of this article (doi:10.1007/s11032-014-0162-8) contains supplementary material, which is available to authorized users.

B. Llorente (✉)
Centre for Research in Agricultural Genomics (CRAG), CSIC-IRTA-UAB-UB, 08034 Barcelona, Spain
e-mail: briardo.llorente@cragenomica.es

B. Llorente · M. M. Flawiá · G. D. Alonso · F. Bravo-Almonacid
Instituto de Investigaciones en Ingeniería Genética y Biología Molecular Dr. Hector N. Torres (INGEBI), Consejo Nacional de Investigaciones Científicas y Técnicas (CONICET), C1428ADN Buenos Aires, Argentina

M. G. López · F. Carrari
Instituto de Biotecnología, Instituto Nacional de Tecnología Agrícola, B1712WAA Castelar, Argentina

R. Asís · R. D. Di Paola Naranjo
Departamento de Bioquímica Clínica, Facultad de Ciencias Químicas, CIBICI-CONICET, Universidad Nacional de Córdoba, X5000HUA Córdoba, Argentina

M. M. Flawiá · G. D. Alonso
Departamento de Fisiología, Biología Molecular y Celular, Facultad de Ciencias Exactas y Naturales, Universidad de Buenos Aires, C1428EGA Buenos Aires, Argentina

F. Bravo-Almonacid
Departamento de Ciencia y Tecnología, Universidad Nacional de Quilmes, B1876BXD Bernal, Argentina

Published online: 10 August 2014

scenarios for modulating the levels of phenolics in crops.

Keywords Chlorogenate · Host plant resistance · Phenylpropanoid metabolism · *Phytophthora infestans* · Polyphenol oxidase · *Solanum tuberosum*

Introduction

The phenylpropanoid metabolic pathway is ubiquitous in land plants (Ferrer et al. 2008). Besides producing phenolic compounds with radical-scavenging activity, this pathway provides vital metabolites for numerous biological processes like vascularization and stem rigidity, flower and fruit volatiles and colors, UV protection, plant–microbe interactions, and plant–pathogen defenses (Dicke and Baldwin 2010; Dixon et al. 2002; Ferrer et al. 2008; Vogt 2010).

A growing body of evidence has highlighted the importance of the phenolic compound chlorogenate in plant defense responses. Overexpression of hydroxycinnamoyl transferase in tomato (*Solanum lycopersicum*) resulted in the accumulation of high levels of chlorogenate, which in turn improved the resistance of the plant to the bacterial pathogen *Pseudomonas syringae* (Niggeweg et al. 2004). Tobacco plants (*Nicotiana tabacum*) overexpressing phenylalanine ammonia-lyase (*PAL*) displayed higher levels of chlorogenate and reduced susceptibility to fungal and oomycete pathogens (Shadle et al. 2003), while plants with suppressed *PAL* expression showed low levels of chlorogenate and reduced basal resistance (Maher et al. 1994; Shadle et al. 2003). Similarly, depletion of substrates from the phenylpropanoid pathway in potato (*Solanum tuberosum*) resulted in plants with decreased levels of chlorogenate and other phenolic compounds that were more susceptible to the oomycete pathogen *Phytophthora infestans*, the causal agent of late blight disease (Yao et al. 1995). Chlorogenate has growth-inhibitory activity upon microorganisms in vitro (Hemaiswarya et al. 2011; Kroner et al. 2011; Lou et al. 2011; Ozcelik et al. 2011; Sung and Lee 2010), and it has also been proposed to interfere with fungal melanin production (Villarino et al. 2011), a process thought to be crucial for plant pathogenicity (Gachomo et al. 2010; Jacobson 2000; Mayer 2006; Steiner and Oerke 2007).

Plant polyphenol oxidases (PPOs) are enzymes with as yet unclear physiological function that catalyze both cresolase [hydroxylation of monophenols to *o*-diphenols; Enzyme Commission [EC] 1.14.18.1] and catecholase (oxidation of *o*-diphenols to *o*-quinones; EC 1.10.3.1) reactions (Thygesen et al. 1995) on several phenolic compounds (Supplementary Fig. 1). Although not considered as part of the phenylpropanoid pathway, potential interactions between PPO and the phenylpropanoid pathway can be reasonably speculated. Certainly, chlorogenate is good substrate for PPO (Martinez and Duvnjak 2006), and clear roles in the biosynthesis of aurones, lignans, and betalains have been proposed for PPO enzymes (Cho et al. 2003; Nakayama et al. 2000; Steiner et al. 1999). Furthermore, recent work has revealed that PPO influences tyrosine and phenylpropanoid metabolism in walnut (Araji et al. 2014).

We previously characterized genetically engineered potato tubers with silenced polyphenol oxidase transcripts (-PPO lines J8, J14, and J20) that accumulated higher amounts of chlorogenate (Llorente et al. 2011). Given the relevance of this compound in plant defense, we investigated the development of late blight disease using our -PPO potato model. We found that -PPO tubers presented improved resistance to the pathogen through a mechanism that appears to involve the accumulation of defensive phenolic compounds via redirection of the phenylpropanoid metabolism.

Materials and methods

Plant and pathogen material

Wild-type (WT) and transgenic (-PPO) potato (*S. tuberosum* var. Spunta) plants (Llorente et al. 2011) were grown in 4-l pots in greenhouses (16-h light/8-h dark photoperiod and 25 ± 3 °C), and tubers were harvested after the aerial parts of the plants had died. The isolate of *P. infestans* (race $R_2R_3R_6R_7R_9$, mating type A2) (Andreu et al. 2006) and the *P. infestans*-GFP strain (Si-Ammour et al. 2003) were kindly provided by Dr. Adriana Andreu (Instituto de Investigaciones Biológicas, Universidad Nacional de Mar del Plata, Argentina) and Dr. Felix Mauch (Department of Biology, University of Fribourg), respectively. Both cultures were maintained on rye agar (Caten and Jinks 1968) at 19 ± 1 °C in the dark with the addition of

5 μg/ml geneticin (Gibco, Billings, MT, USA) to the *P. infestans*-GFP culture media.

Pathogen inoculation and quantification

After 10 days of growth, pathogen mycelia were harvested in 25 ml sterile water and stimulated to release zoospores by incubation at 4 °C for 5 h. Following filtration through a 15-μm nylon filter cloth, zoospores and sporangia suspension were examined under a light microscope for quantification and the concentration was adjusted to 25 sporangia/μl to be used as an inoculum. Four-month-old tuber discs (8,000 μm diameter × 1,000 μm thick) were inoculated in the center with 10 μl of water (mock-inoculated controls) or 10 μl of inoculum and maintained into a plastic box at 19 ± 1 °C in the dark. The disease progression was monitored for 6 days using a quantitative polymerase chain reaction (qPCR) method as previously described (Llorente et al. 2010) with the modification that the efficiency-based comparative quantification analysis method (McCurdy et al. 2008), integrated in the Rotor-Gene 6000 software (Corbett Life Science, Mortlake, NSW, Australia), was used. Briefly, potato DNA and *P. infestans* DNA were simultaneously extracted from inoculated potato tissue, and the pathogen relative abundance was quantified using SYBR Green technology and a Rotor-Gene 6000 instrument (Corbett Life Science, Mortlake, NSW, Australia) by normalizing the value obtained from the *P. infestans PiO8* high-copy-number DNA target sequence (Judelson and Tooley 2000) and the corresponding value from the elongation factor 1-α gene of *S. tuberosum* (*Ef-1α*: AB061263.1) for each individual sample. Disease progression data were obtained from 16 to 20 biological replicates per time point. Three technical replicates were performed, and the mean values were used for further calculations. All data were normalized to the mean value obtained for WT samples at 6 days after inoculation (DAI), which was set at 100 %.

In silico screening for potential host-induced gene silencing in *P. infestans*

Potential sequence homology between the hairpin sequence introduced in the -PPO potato plants and *P. infestans* genes was evaluated by searching in the Broad Institute of Harvard and Massachusetts Institute of Technology (MIT) database (http://www.broadinstitute.org/annotation/genome/phytophthora_infestans/MultiHome.html) and in the National Center for Biotechnology Information (NCBI) database (http://blast.ncbi.nlm.nih.gov/) using nucleotide BLAST.

Microscopic examinations

Tuber discs (2,500 μm thick) of 7 DAI were used for microscopic examinations. Central portions of the discs were transversally sliced into 250-μm-thick layers with a Vibratome Sectioning System Series 1000 (Vibratome, St. Louis, MO, USA). Confocal microscopy was performed with a Nikon C1 confocal microscope (Nikon, Tokio, Japan) using excitation at 488 nm (Argon blue laser) and 544 nm (Helium–Neon green laser) and collecting emitted light from 500 to 600 nm. Real color 3D surface plots in Supplementary Fig. 2 were obtained using ImageJ 1.44o program (http://imagej.nih.gov/ij/).

Metabolic profiling

Tuber samples (4–8 individual batches of samples pooled from 25 plants per condition) were collected at 2 DAI, frozen in liquid nitrogen, and stored at −80 °C until further analysis. Extractions were performed by grinding the tissue in liquid nitrogen and addition of the appropriate extraction solution. Levels of starch, sucrose, fructose, and glucose were determined as described by Fernie et al. (2001). The levels of all other metabolites were quantified by gas chromatography coupled to mass spectrometry (GC–MS) as previously described (Llorente et al. 2011), and chlorogenate levels were confirmed by high-performance liquid chromatography coupled to mass spectrometry (HPLC–MS).

Chlorogenate HPLC–MS quantification was performed using filtered (0.45 μm) lyophilized samples dissolved in 0.5 % formic acid/methanol (1:1, v/v) using filters HAWG04756 (Millipore, São Paulo, Brazil), HPLC grade methanol (J.T. Baker, Edo. de México, México), and puriss. p.a. for mass spectroscopy formic acid (Fluka, Steinheim, Germany). Ultrapure water (<5 μg/l TOC) was obtained from a purification system, Arium 61316-RO plus Arium 611 UV (Sartorius, Goettingen, Germany). All

samples were analyzed in duplicate by HPLC–DAD–ESI–MS/MS method, using an Agilent Technologies 1200 Series system (Agilent Technologies, Santa Clara, CA, USA) equipped with a gradient pump (Agilent G1312B SL Binary), solvent degasser (Agilent G1379 B), and autosampler (Agilent G1367 D SL+WP). The chromatographic separation was achieved on a LUNA (Phenomenex, Torrance, CA, USA) reversed-phase C18 column (5 μm, 250 mm × 4.60 mm i.d.). The column temperature was thermostated at 35 °C using a column heater module (Agilent G1316 B). The mobile phase consisted of 0.5 % formic acid in ultrapure water (v/v, solvent A) and 0.5 % acid formic in methanol (v/v, solvent B), starting with 20 and changing to 50 % B during 3 min, kept for 5 min, followed by a second ramp to 70 % B in 7 min, maintained for 5 min, a third ramp to 80 % B in 1 min, maintained for 9 min, remaining at this last condition for 10 min before next run. The flow rate was 0.4 ml/min, injecting 40 μl on column. The HPLC system was connected to a photodiode array detector (Agilent G1315 C Satarlight DAD) and subsequently to a micrOTOF-Q11 Series QTOF mass spectrometer (Bruker, Billerica, MA, USA) equipped with an electrospray ionization (ESI) interface. UV–Vis spectra were registered from 200 to 600 nm. Mass spectra were recorded in negative ion mode between *m*/*z* 50 and 1,000. The working conditions for the ionization source were as follows: capillary voltage, 4,500 V; nebulizer gas pressure, 4.0 bar; drying gas flow, 8.0 l/min; and drying gas temperature, 180 °C. Nitrogen and argon were used as nebulizer and collision gases, respectively. The MS detector was programmed to perform an MS/MS scan of the three most abundant ions, using collision energy of 13.0 eV. Identification was based on UV–Vis spectra, retention time, and mass spectra, as compared with a commercial chlorogenate standard (Sigma-Aldrich, Steinheim, Germany). In the MS spectrum obtained for this compound, a molecular ion at *m*/*z* 353 was observed, yielding signal at *m*/*z* 191 in the MS/MS analysis. Quantification was performed from the peak areas by reference to calibration curves obtained using the chlorogenate standard at concentrations between 0.78 and 100 μg/ml. Wavelength used for quantification was 320 nm. The Compass version 3.1 software and DataAnalysis version 4.0 software were used for data acquisition and processing, respectively.

PPO activity

Protein extracts were obtained from tuber tissue homogenized at a ratio of 200-mg fresh weight to 1-ml homogenization solution [50 mM Tris–HCl, pH 7.5, 2 mM β-Me, 0.1 mM PMSF, 1 μg/ml leupeptin, 3 % (w/v) PVPP, and 1 mM Na_2 EDTA, 20 % glycerol]. The homogenate was centrifuged at 10,000×*g* at 4 °C for 20 min, and the supernatant was used for protein quantification and assessment of PPO activity. Total protein was quantified by the Bradford method (Bradford 1976), using bovine serum albumin as standard. PPO activity assays were performed with 2 μg protein extracts in 1,000 μl of 20 mM phosphate buffer (pH 6) containing 4 mM $MgCl_2$ and 10 mM L-DOPA. PPO activity was followed by the change in absorbance at 475 nm due to the oxidation of L-DOPA.

Gene expression analysis

Total RNA was extracted using Trizol reagent (Invitrogen, Carlsbad, CA, USA) according to the manufacturer's instructions. Purified RNAs were quantified by spectroscopy using a NanoDrop apparatus (Thermo Scientific, MA, USA), and RNA integrity was evaluated by agarose gel electrophoresis. RNA samples were treated with RNase-free DNase I (Promega, Fitchburg, WI, USA) according to the manufacturer's instructions, and cDNA was generated with the Superscript III Reverse Transcriptase Kit (Invitrogen, Carlsbad, CA, USA) according to the manufacturer's instructions, using random primers plus 2 μg of total RNA. The relative mRNA abundance was evaluated via quantitative reverse transcription PCR (RT-qPCR) in a total reaction volume of 20 μl using LightCycler 480 SYBR Green I Master (Roche, Basel, Switzerland) on a LightCycler 480 Real-Time PCR System (Roche, Basel, Switzerland) with 0.3 μM of each specific sense and antisense primers. The mRNA abundance of the *PPO* gene family members *POT32* (U22921), *POT33* (U22922), and *NOR333* (M95196) was simultaneously monitored using the primers CuDomPPO Fwd and CuDomPPO Rev that amplify a conserved region of the copper-binding domain A of PPO (Thygesen et al. 1995). Defense signaling pathways were examined by quantifying the mRNA abundance of *PR-1* (*S. tuberosum* pathogenesis-related protein group 1), *ChtA* (*S. tuberosum* acidic chitinase A class II), *ChtB4* (*S. tuberosum* basic chitinase B4), *Drd-1* (*S. tuberosum* defense-related alcohol/$NADP^+$ oxido-

reductase), *PAL* and *C4H* (*S. tuberosum* cinnamate 4-hydroxylase). *EF-1α* was used as an endogenous control because it has been validated to be a suitable gene for RT-qPCR gene normalization expression in potato (Nicot et al. 2005; Orlowska et al. 2012). *PR-1* and *ChtA* genes were measured using primers previously described (Orlowska et al. 2012). Information about the other primers used in RT-qPCR analyses is described in detail in Supplementary Table 2. Cycling conditions were 95 °C for 10 min followed by 45 cycles of 10 s at 95 °C, 30 s at 60 °C, and a final melting curve ramping from 65 to 95 °C. Three independent biological replicates of each sample were used. Two technical replicates of each biological replicate were performed, and the mean values were considered for further calculations. The normalized expression was calculated as described by Simon (2003) using *EF-1α* as the endogenous reference gene. Fold change values are reported relative to mock-inoculated WT expression levels.

Data analysis

One-way ANOVA followed by Newman–Keuls multiple comparison post hoc tests was used to determine statistical significance in the qPCR pathogen abundance determination. Heat maps were performed on the $\log_2$-transformed metabolite data using the Multiexperiment Viewer version 10.2 program (http://www.tm4.org/mev/) (Do et al. 2010). Statistical significance in chlorogenate contents, PPO activity, and mRNA abundance was determined by one-way ANOVA followed by the Newman–Keuls multiple comparison test or by the *t* test. Pearson's correlation coefficients (*r* values) were calculated using the means of metabolite concentrations and PPO activity. Statistical analysis was performed using GraphPad Prism 5.0a (GraphPad Software, La Jolla, CA, USA). Metabolite content variations in Supplementary Fig. 3 were assessed by the *t* tests analysis using EXCEL (Microsoft Corporation, Redmond, WA, USA).

Results

Phytophthora infestans invasiveness is reduced in -PPO lines

To assess whether PPO knockdown lines exhibited altered disease resistance, WT and -PPO tubers inoculated with *P. infestans* were evaluated for pathogen invasiveness (defined as the capacity of a pathogen to grow and spread within the host) (Cabrefiga and Montesinos 2005) by quantifying the level of infection using a qPCR method (Llorente et al. 2010). The infection resulted in similar relative *P. infestans* abundance in the WT and transgenic lines during the first 4 DAI. However, a significant ($P \leq 0.05$) reduction was detected in all transgenic lines when compared to WT controls at 5 and 6 DAI (Fig. 1).

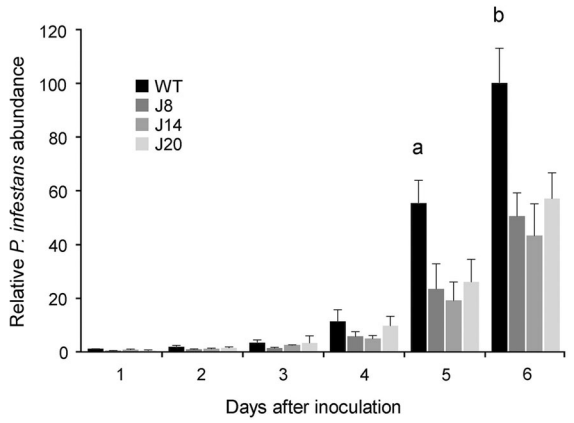

Fig. 1 *Phytophthora infestans* growth in WT and transgenic (-PPO: J8, J14, and J20) tuber tissue. Relative pathogen abundance was determined by quantitative PCR from 1 to 6 DAI. No significant differences were found among lines the first 4 DAI, but WT controls presented significantly ($P \leq 0.05$) higher relative pathogen abundance than PPO lines at 5 and 6 DAI according to one-way ANOVA followed by the Newman–Keuls multiple comparison test (indicated with *lowercase letters a* and *b*, respectively). The mean value for WT at 6 DAI was set at 100 %. *Error bars* represent the ± SEM of 16–20 individual samples

We tested the hypotheses that the resistant phenotype was a consequence of host-induced gene silencing (HIGS) (Nowara et al. 2010), changes in defense signaling pathways or altered phenolics-mediated response against *P. infestans*. By surveying the *P. infestans* genome databases of the Broad Institute and the NCBI, we looked for matching sequences to the *PPO* gene silencing hairpin introduced in the -PPO lines (Llorente et al. 2011). This survey identified three potential off-target silencing sequences of 11–15 nucleotides in length corresponding to the NADH dehydrogenase subunit 1 gene, the *NUK7* gene, and the retrotransposon copia-like PICR2 (Supplementary Table 1). Because the identified sequences are shorter than the conserved minimum length required (20–25

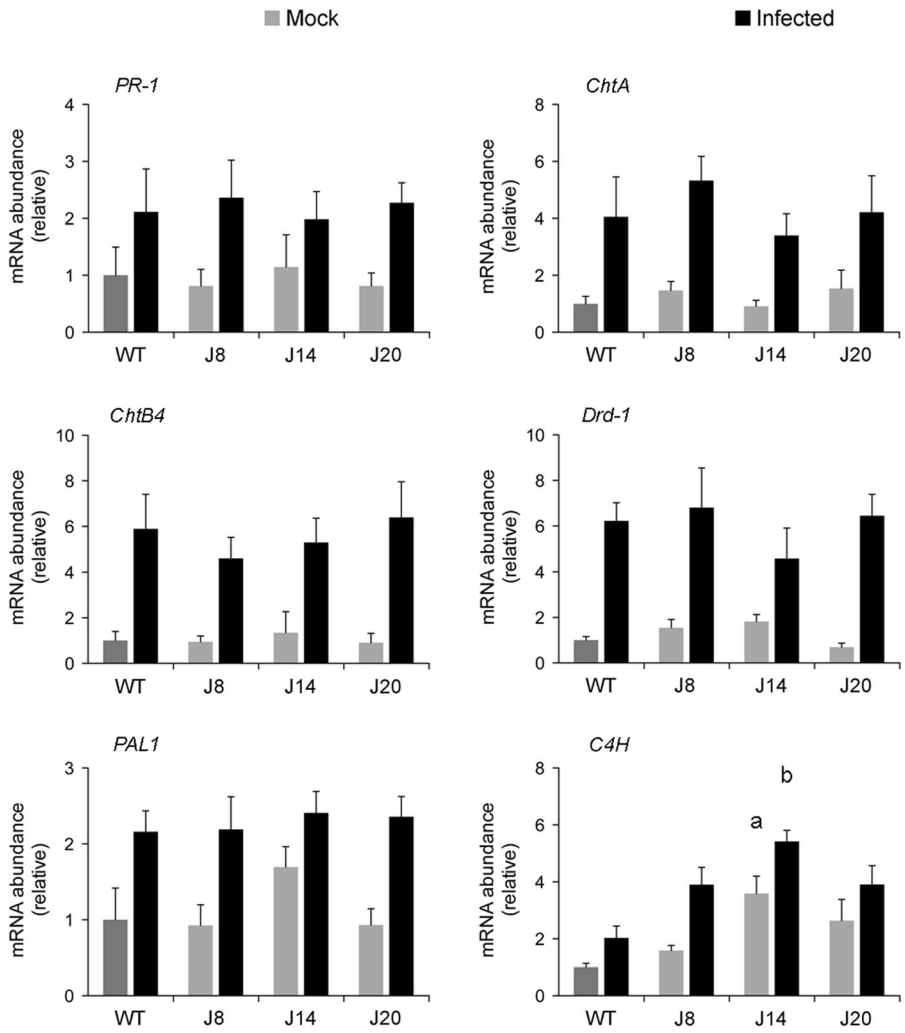

Fig. 2 Relative expression profiles of examined defense-related genes. Samples were analyzed at 2 days after inoculation. *PR-1* pathogenesis-related protein group 1, *ChtA* acidic chitinase A, *ChtB4* basic chitinase B4, *Drd-1* defense-related alcohol/NADP$^+$ oxido-reductase, *PAL1* phenylalanine ammonia-lyase 1, *C4H* cinnamic acid 4-hydroxylase. Differences in mRNA abundance were only significant for *C4H* in J14 samples over both mock-inoculated and infected WT samples (indicated with *lowercase letters a* and *b*, respectively). Values are normalized to those obtained for *EF-1α* and are expressed as relative mRNA abundance compared to mock-inoculated WT. Mock-inoculated and *P. infestans*-inoculated samples are represented as *gray* and *black bars*, respectively. Statistical significance ($P \leq 0.05$) was assessed with the one-way ANOVA followed by the Newman–Keuls multiple comparison test. The values are mean ± SEM of three biological replicates

nucleotides) for triggering RNA-dependent gene silencing in eukaryotes (Chapman and Carrington 2007; Liu and Paroo 2010), we excluded the HIGS hypothesis from further analyses.

Considering that early plant responses are believed to be critical in determining the fate of late blight disease progression (Orlowska et al. 2012) and that the relative pathogen abundance at 2 DAI was comparable in all samples (Fig. 1), we chose this time point to analyze the expression of well-characterized defense-related genes as a control for altered defense signaling pathways. We examined the expression of (1) *PR-1*, a salicylic acid (SA) pathway-dependent marker; (2) *ChtA*, a marker for systemic acquired resistance (SAR) (Buchter et al. 1997; Hoegen et al. 2002; Orlowska et al. 2012; Payne et al. 1988); (3) *ChtB4*, an ethylene (ET) signaling gene marker (Beerhues and Kombrink 1994; Montesano et al. 2005); (4) *Drd-1*, a responsive

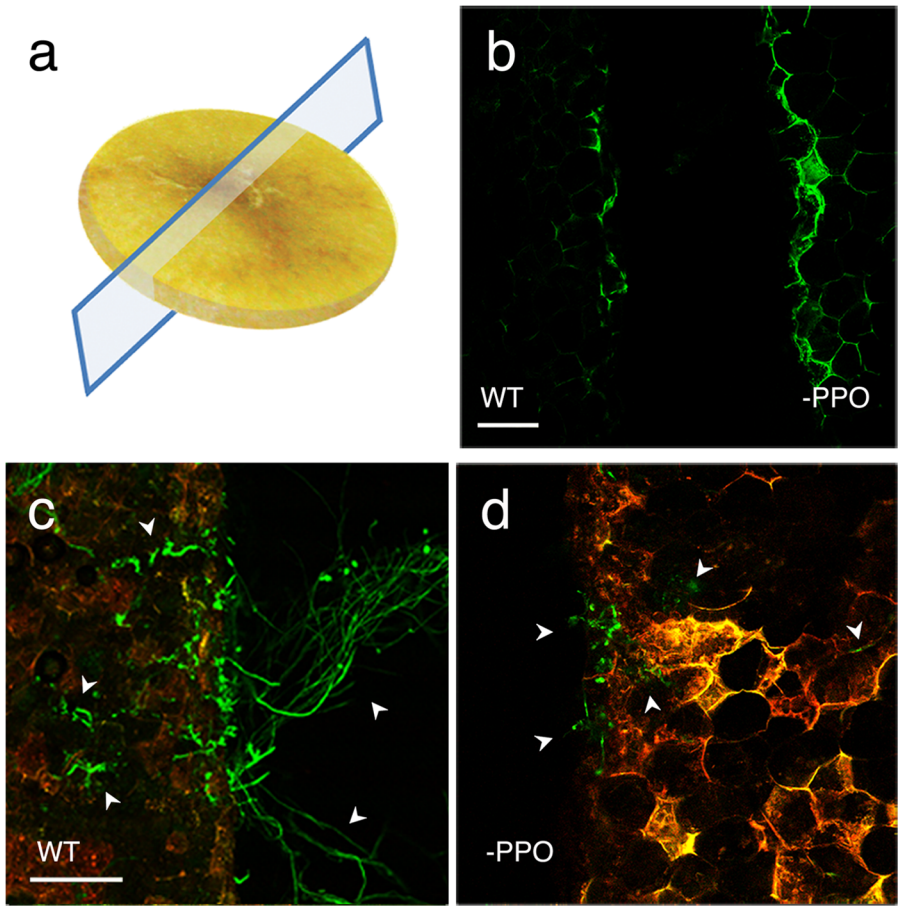

Fig. 3 Microscopic analyses of WT and -PPO tuber tissue inoculated with *P. infestans*. **a** Schematic representation of the microscopic cross-sectional views. **b** Confocal microscopy of WT and -PPO samples showing differential accumulation of autofluorescent phenolic compounds. The image was obtained using Argon blue laser excitation (488 nm), under which plant autofluorescent phenolics look *green*. **c** Confocal microscopy of WT potato tissue infected with *P. infestans*-GFP. **d** Confocal microscopy of -PPO potato tissue infected with *P. infestans*-GFP. *Arrowheads* in **c**, **d** indicate *P. infestans* hyphae. **c**, **d** Merge images obtained with Argon blue (488 nm) and Helium–Neon green lasers (544 nm), under which plant autofluorescent phenolics look *yellow-orange* and *P. infestans*-GFP looks *green* (for detailed description, see also Supplementary Fig. 2). *Scale bar* 200 μm

marker for jasmonates (JA), ET, and SA (Montesano et al. 2003, 2005); and (5) *PAL* and *C4H*, coding for the enzymes that catalyze the first and second steps of the phenylpropanoid pathway, respectively (Ferrer et al. 2008). Analogous mRNA abundance patterns were obtained both for WT and transgenic lines, with the exception of *C4H* that was generally expressed at higher levels in the -PPO lines (Fig. 2), therefore suggesting possible changes in phenylpropanoid metabolism.

Given that the induction of phenylpropanoids involved in defense responses can be identified by a characteristic cellular autofluorescence under UV-blue light illumination (Bennett et al. 1996; Huckelhoven 2007; La Camera et al. 2004; Yao et al. 1995), we microscopically examined both WT- and -PPO-infected tuber disc cross sections (Fig. 3a). At 7 DAI, infected -PPO tuber samples presented a clearly stronger autofluorescence than WT samples, originated from plant phenolic compounds (Fig. 3b). To gain a better understanding of this response, additional experiments were performed using a *P. infestans* strain that constitutively express the green fluorescent protein (*P. infestans*-GFP) (Si-Ammour et al. 2003). Experiments using the *P. infestans*-GFP strain also evidenced a stronger autofluorescence in the

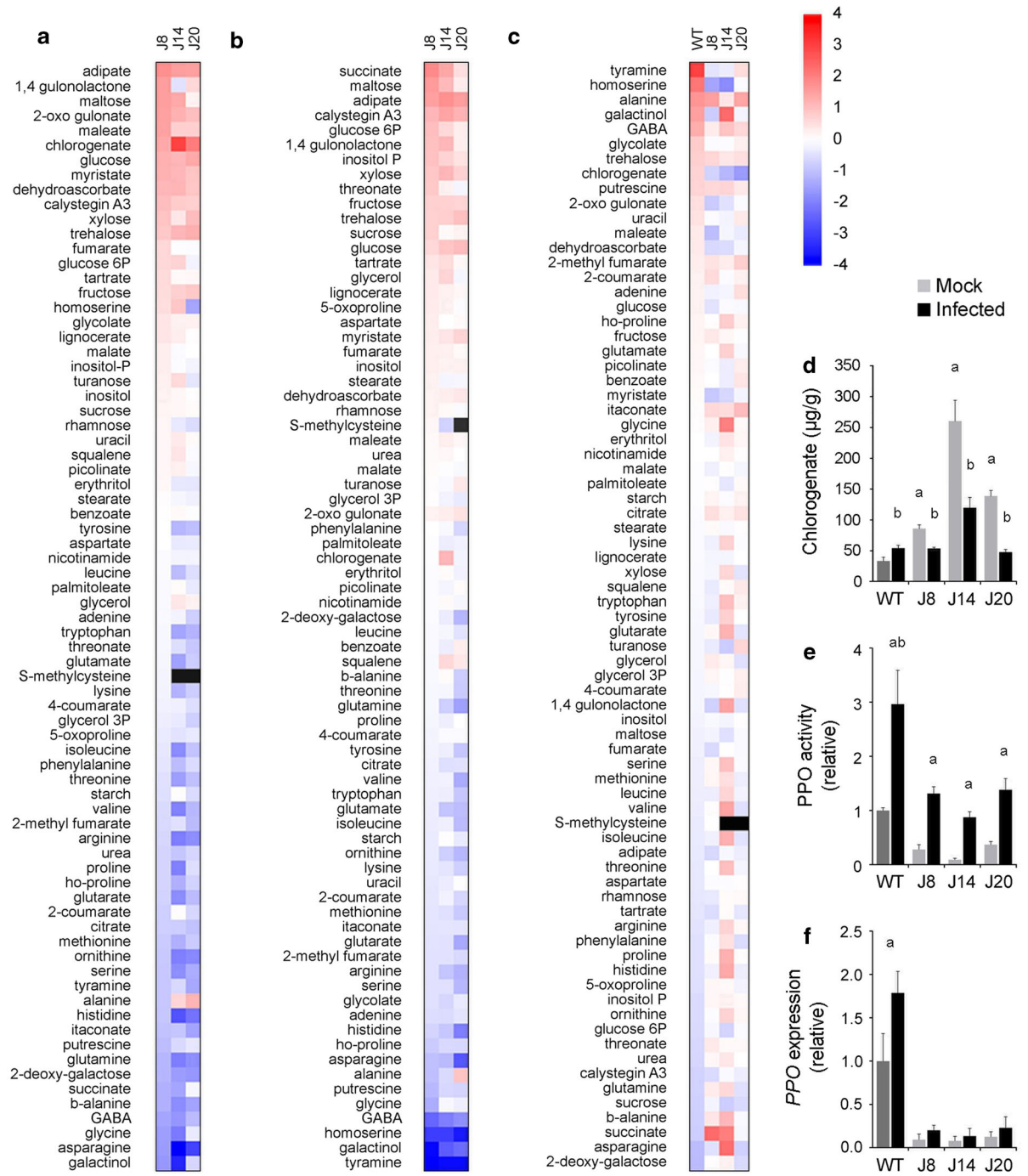

transgenic tissue (compare Fig. 3c, d). These results suggested that an altered phenolics-mediated defense response in -PPO cells was responsible for the reduced invasiveness of *P. infestans*.

Plant metabolite profiling of late blight infection

Late blight disease symptoms are commonly first observed after 2 DAI (Fry 2008; Halim et al. 2007;

◀**Fig. 4** Metabolic analyses of WT and -PPO tuber tissue inoculated with *P. infestans*. **a** Heat map visualization of metabolites changes in -PPO plant lines. Fold change was obtained comparing metabolite levels of mock-inoculated -PPO lines to mock-inoculated WT. **b** Heat map visualization of metabolites changes due to infection in -PPO lines compared to WT plants. Fold change was obtained comparing metabolite levels of infected -PPO lines to infected WT. **c** Heat map visualization of metabolites changes due to infection. Fold change was obtained comparing metabolite levels of each infected line to their corresponding mock-inoculated counterpart. Each *colored dot* represents the effect on metabolite level in comparison with the corresponding control using a *false-color scale*. Values represent the $\log_2$-transformed metabolite data considering 0 as no change value with respect to the comparison control (*white squares*). Increased metabolite contents are displayed in *red*. Decreased metabolite contents are displayed in *blue*. Non-detected metabolites are displayed in *black*. Metabolites fold variations are given in Supplementary Fig. 3. **d** HPLC–MS detailed chlorogenate contents. All mock-inoculated -PPO samples presented significant increments over mock-inoculated WT samples (indicated with *lowercase letter a*). All lines presented significant differences between mock-inoculated and the corresponding infected samples (indicated with *lowercase letter b*) according to the *t* test. **e** PPO activity. All infected samples presented significant increments than the corresponding mock-inoculated samples (indicated with *lowercase letter a*). PPO activity was significantly higher in infected WT samples than in infected -PPO samples (*indicated with lowercase letter b*). **f** Levels of *PPO* transcripts. Significant differences were only detected between mock-inoculated and infected WT samples (indicated with *lowercase letter a*). In **d–f,** mock-inoculated and *P. infestans*-inoculated samples are represented as *gray* and *black bars*, respectively. If not specified, statistical significance ($P \leq 0.05$) was assessed with the one-way ANOVA followed by the Newman–Keuls multiple comparison test. Data in **e**, **f** are presented as the relative values compared to the mock-inoculated WT. *Error bars* represent the ± SEM from 6 to 8 (**d**), 4 to 6 (**e**), and 3 (**f**) individual samples per condition

Llorente et al. 2010) and correlate with the formation of infectious structures (haustoria) (Haas et al. 2009). On the basis of these observations, and given that the relative pathogen abundance at 2 DAI was not significantly different in WT and -PPO lines (Fig. 1), samples at 2 DAI were profiled for the relative contents of primary and few targeted secondary metabolites to characterize in deep the defense response against *P. infestans*.

Data presented in Fig. 4a show that transgenesis had a major impact over plant metabolism when compared to WT controls. A minor fraction of detected compounds increased their levels in the transgenic lines, including fatty acids, sugars, and few intermediates of aromatic amino acids and phenylpropanoid metabolism, particularly chlorogenate. On the other hand, two intermediates of the phenylpropanoid metabolism, 4- and 2-coumarate, showed lower levels in the transgenic lines. Markedly, a deep reduction in the level of many amino acids was detected. From the 27 quantified amino acids, 21 showed decreased levels and the remaining 6 exhibited different behaviors: s-methylcysteine could only be quantified in line J8; aspartate, leucine, and tyrosine were decreased in lines J14 and J20 without content changes in line J8, while alanine and homoserine exhibited increased levels in lines J14 and J20, and J8 and J14, respectively.

The combined analysis of transgenesis and infection effects revealed similar metabolic alteration to those observed owing to transgenesis (Fig. 4b). However, some metabolites displayed different accumulation patterns due to infection in the transgenic lines when compared against the infected WT controls. Succinate, threonate, and 5-oxoproline, which decreased in the mock-inoculated -PPO lines, showed increased levels as a consequence of the infection. On the other hand, the levels of glycolate, homoserine, and uracil, which were higher in the mock-inoculated samples, diminished because of the pathogen infection. Notably, there were a group of metabolites that either decreased or increased due to transgenesis that reached similar levels to those of mock-inoculated WT controls as a consequence of the infection. Among them, glycerol-3P, phenylalanine, tyrosine, and urea had lower levels, while chlorogenate and maleate displayed higher accumulation in -PPO lines compared to WT samples when mock-inoculated plants were analyzed (Fig. 4a). Finally, aspartate and adenine exhibited the same levels in transgenic and WT mock-inoculated samples (Fig. 4a) but the infection caused an increase in aspartate and a decrease in adenine in -PPO lines (Fig. 4b).

In order to distinguish the effects triggered by the infection from those originated from the transgenesis, the metabolite contents of the infected samples were compared to those of their mock-inoculated counterparts (Fig. 4c). Out of the 75 metabolites quantified, 16 displayed differential accumulation patterns between WT and -PPO lines due to *P. infestans* infection. These metabolic alterations can be categorized into six different behaviors: (1) infection caused a decrease in WT plants but an increase in the transgenics (this was the case of the TCA cycle

intermediate succinate); (2) infection caused a decrease in WT plants without altering the levels in the transgenics (urea, threonate, inositol-P, 5-oxoproline); (3) infection caused no alteration in WT plants but an increase in the transgenics (citrate, itaconate); (4) infection caused no alteration in WT plants but a decrease in the transgenics (myristate); (5) infection caused an increase in WT plants and a decrease in the transgenics (glucose, dehydroascorbate, maleate, 2-oxogulonate, chlorogenate, homoserine, and tyramine); (6) Infection caused an increase in WT plants but no alteration in the transgenics (glycolate).

Metabolites related to the phenylpropanoid pathway demonstrated the largest changes between WT and -PPO cells under pathogen attack

The phenylpropanoid chlorogenate was the metabolite with the highest increase in -PPO lines (Fig. 4a). Detailed examination showed that all mock-inoculated -PPO samples presented significantly ($P \leq 0.05$) higher amounts (2.5-fold–7.5-fold) of chlorogenate than their WT controls (Fig. 4d) that inversely correlated with PPO activity ($r = -0.87$) (Fig. 4d, e). While the PPO activity increased significantly ($P \leq 0.05$) in all infected samples compared to mock-inoculated controls, the WT-infected samples presented an approximately threefold higher PPO activity than the -PPO-infected ones (Fig. 4e). However, no significant modifications between mock-inoculated and infected samples were detected in -PPO lines when *PPO* gene expression was analyzed via a quantitative reverse transcription PCR (RT-qPCR) designed to simultaneously monitor all *PPO* gene family members expressed in tubers (Fig. 4f).

In order to better interpret the impact of *P. infestans* infection over plant metabolism, a set of metabolic map schemes were drawn to simplify the comparison of metabolite levels behavior. This analysis clearly revealed that the cluster of metabolites related to the phenylpropanoid pathway was the one that presented the largest and most generalized differences between WT and -PPO cells under *P. infestans* attack (Fig. 5).

Discussion

In previous work, we characterized PPO-silenced potato lines (-PPO) that presented tubers with higher chlorogenate content than WT plants (Llorente et al. 2011), raising the question of whether these transgenic lines might also be more resistant to pathogens. In this work, we explored this hypothesis and evaluated the susceptibility of -PPO potato tubers to the oomycete pathogen *P. infestans*.

The invasiveness of *P. infestans* was reduced in -PPO tubers, as a delayed progression of the infection was observed when compared to WT controls (Fig. 1). We excluded the HIGS hypothesis because, even if the available information concerning the *P. infestans* RNA-silencing machinery is limited (Ah-Fong et al. 2008; Whisson et al. 2005), it can be speculated that the length of the off-target identified sequences (Supplementary Table 1) might not be enough to efficiently trigger HIGS events that could negatively affect the growth of *P. infestans*. Analysis of defense-related gene expression (Fig. 2) suggested that the reduced invasiveness of the pathogen in the -PPO tissue was likely not a consequence of altered defense signaling pathways. However, the induction of the *C4H* gene (Fig. 2) has also been observed in PPO-silenced walnut plants (Araji et al. 2014) and could be the consequence of regulatory mechanisms acting on the phenylpropanoid metabolism due to the silencing of PPO.

The autofluorescence signal originating from the plant cells in the transgenic tissue (Fig. 3) is consistent with several previous works demonstrating plant resistance to pathogens mediated by phenolic compounds (Bennett et al. 1996; Huckelhoven 2007; La Camera et al. 2004; Yao et al. 1995). In accordance, the results of the targeted metabolite profile analysis indicated alterations in the metabolite concentrations from phenylpropanoid precursors to downstream phenylpropanoid products (Figs. 4a, 5a): tyrosine as well as phenylalanine contents inversely correlated ($r = -0.77$ and $r = -0.99$, respectively) with chlorogenate contents in -PPO lines. This inverse correlation in the content of precursors and end products has been previously described for the phenylpropanoid pathway in potato (Payyavula et al. 2012, 2013). Based on the obtained results and very recent findings demonstrating a direct role for PPO in the metabolism of tyrosine (Araji et al. 2014), we speculate that the reduction of the PPO-catalyzed reaction on tyrosine redirects the metabolic flux into the phenylpropanoid pathway, resulting in increased accumulation of chlorogenate in the PPO-silenced lines. Additionally,

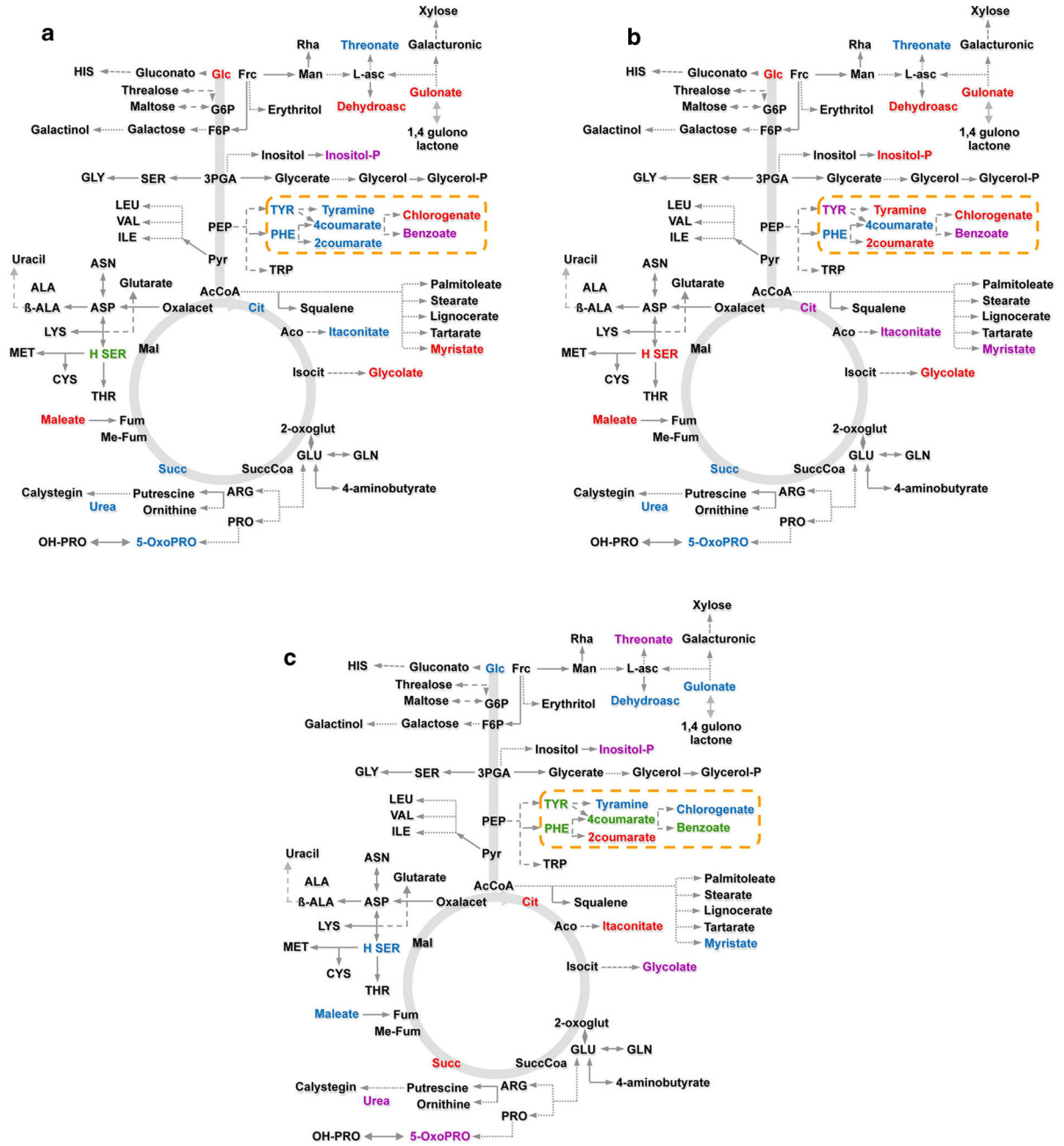

Fig. 5 Schematic representations of differential metabolic changes caused by *P. infestans* infection. **a** Metabolite level variations in mock-inoculated -PPO lines compared to mock-inoculated WT. **b** Metabolite level variations in infected WT compared to mock-inoculated WT. **c** Metabolite level variations in infected -PPO lines compared to their corresponding mock-inoculated counterparts. Metabolites marked in *red* or *blue* indicate increase or decrease in metabolite level, respectively. Metabolites marked in *violet* and *green* indicate no change and variability in metabolite level, respectively. Metabolites in *black* were not affected by *P. infestans* infection. Metabolites related to the phenylpropanoid pathway are framed by *orange dashed-line squares*

the lack of PPO activity could also contribute to accumulate higher amounts of free chlorogenate in -PPO cells.

The increase in chlorogenate levels observed in WT tubers during the infection is a clear plant defense response, although this induction does not reach the levels found in transgenic lines (Fig. 4d). Thus, the higher levels of chlorogenate in -PPO cells could be acting as a phytoanticipin (VanEtten et al. 1994), as previously established (Leiss et al. 2009; Niggeweg et al. 2004; Shadle et al. 2003; Villarino et al. 2011; Yao et al. 1995). While Niggeweg et al. (2004) reported that an 85 % increase in chlorogenate content was sufficient to impart enhanced pathogen resistance, we found a 2.5-fold–7.5-fold higher accumulation in the contents of this metabolite in the -PPO lines (Fig. 4d). On the basis of in vitro studies, chlorogenate has been proposed to impart its antimicrobial activity by disrupting the structure of the pathogen enzymes and cell membrane through direct binding (Hemaiswarya et al. 2011; Lou et al. 2011; Sung and Lee 2010). The dramatic reduction in soluble chlorogenate contents observed in the infected -PPO lines (Fig. 4d) fits with the above-described mechanism of action and strongly supports the idea that this metabolite was used to counteract the *P. infestans* invasion.

It has been recently suggested that tyramine may be directly metabolized by PPO in walnut (Araji et al. 2014). Notably, we observed a strikingly different trend in tyramine levels in PPO-silenced potato lines to that found in PPO-silenced walnut plants. While downregulation of PPO in walnut caused an accumulation of tyramine (Araji et al. 2014), this metabolite was reduced in -PPO tubers (Fig. 4a). Furthermore, tyramine levels increase in WT tubers but decrease in PPO-silenced lines in response to pathogen infection (Fig. 4c). The reason for this is as yet unknown; however, the reduced levels of tyrosine (which is the precursor of tyramine) in -PPO tubers (Fig. 4a) could be altering tyramine metabolism in these lines. The different tissues analyzed (leaves in walnut and tubers in potato) could also account for the aforementioned differences. Additionally, the different number of PPO-coding genes in walnut (one) (Araji et al. 2014) and potato (at least six) (Thygesen et al. 1995) could imply alternative PPO-dependent tyramine metabolism in these species.

The increase in PPO activity in all infected samples (Fig. 4e), along with the lack of substantial differences in *PPO* gene expression between infected and mock-inoculated -PPO samples (Fig. 4f), could be explained by the fact that microorganisms are able to detoxify phenolic compounds thanks to enzymes similar to PPO (Hernandez-Romero et al. 2005; Lyr 1962; Nikitina et al. 2010; Pinero et al. 2007; Yang and Chen 2009). The former observation further suggests that these measurements may include the combined activities of both plant and pathogen oxidases.

Besides the evident changes in phenylpropanoid metabolism, other factors contributing to plant defense cannot be ruled out. For example, the marked reduction in the level of many amino acids in transgenic tubers could also represent a significant factor affecting the growth dynamics of *P. infestans* since it has been inferred that this pathogen may utilize the free amino acids of tubers as a major carbon source to grow during infection (Judelson et al. 2009).

Our study corroborates and provides a molecular explanation to comparable results reported in a Monsanto patent (Hakimi et al. 2006) describing enhanced resistance to *P. infestans* in PPO-downregulated potato tubers. On the other hand, our results differ from a previous work (Rommens et al. 2006) reporting no evident lesion size differences between a PPO-silenced line and Ranger Russet WT tubers infected with *P. infestans* (US-8 strain). However, these results are not necessary in conflict since differences originated from the method used to determine *P. infestans* disease progression, namely lesion size determination opposed to qPCR pathogen abundance quantification, have been previously reported (Halim et al. 2007; Yu et al. 1997). Our results contrast with previous work where PPO activity in tomato and dandelion (*Taraxacum officinale*) plants was correlated with reduced susceptibility to the bacteria *P. syringae* pv. tomato (Li and Steffens 2002; Richter et al. 2012; Thipyapong et al. 2004a). The origin of these discrepancies is unclear, but could be inherent in the use of different pathosystems.

Together, our results suggest that PPO downregulation mainly contributes to accumulate phenolic compounds in the plant cells by redirecting the metabolic flux from phenylpropanoid precursors to phenylpropanoid end products, creating unfavorable conditions to *P. infestans* growth. Interestingly, this hypothesis also allows explaining why transgenic tomato plants with reduced PPO activity have increased drought tolerance (Thipyapong et al. 2004b) and why some plants decrease their PPO

activity while encountering stress conditions (Balakumar et al. 1997; Ben Ahmed et al. 2009, 2010; Rivero et al. 2001). Probably, as also noted by Balakumar et al. (1997), allowing the plant to accumulate higher levels of antioxidant phenolic compounds used to reduce oxidative stress damage during harsh conditions. The presented results emphasize the importance of components acting in parallel to canonical metabolic pathway constituents in influencing plant metabolism and open new scenarios to modify the content of phenolics in crops.

Acknowledgments We thank A. Andreu and F. Mauch for kindly providing the *P. infestans* and *P. infestans*-GFP strains, respectively. We thank C. Cvitanich and E. Orlowska for valuable experimental advice, and also M. A. Phillips, M. E. Segretin, and D. Caparrós-Ruiz for their critical analysis of the manuscript. This work was funded by Consejo Nacional de Investigaciones Científicas y Técnicas (CONICET), Facultad de Ciencias Exactas y Naturales (FCEyN), Universidad de Buenos Aires (UBA), and Agencia Nacional de Promoción Científica y Tecnológica (ANPCyT), Argentina. Additional support was received from Coimbra Group and Wood-Whelan research fellowships from the International Union of Biochemistry and Molecular Biology (IUBMB).

References

Ah-Fong AM, Bormann-Chung CA, Judelson HS (2008) Optimization of transgene-mediated silencing in *Phytophthora infestans* and its association with small-interfering RNAs. Fungal Genet Biol 45:1197–1205

Andreu AB, Guevara MG, Wolski EA, Daleo GR, Caldiz DO (2006) Enhancement of natural disease resistance in potatoes by chemicals. Pest Manag Sci 62:162–170

Araji S et al (2014) Novel roles for the polyphenol oxidase enzyme in secondary metabolism and the regulation of cell death in walnut. Plant Physiol 164:1191–1203

Balakumar T, Gayathri B, Anbudurai PR (1997) Oxidative stress injury in tomato plants induced by supplemental UV-B radiation. Biol Plant 39:215–221

Beerhues L, Kombrink E (1994) Primary structure and expression of mRNAs encoding basic chitinase and 1,3-beta-glucanase in potato. Plant Mol Biol 24:353–367

Ben Ahmed C, Ben Rouina B, Sensoy S, Boukhriss M, Ben Abdullah F (2009) Saline water irrigation effects on antioxidant defense system and proline accumulation in leaves and roots of field-grown olive. J Agric Food Chem 57:11484–11490

Ben Ahmed C, Ben Rouina B, Sensoy S, Boukhriss M, Ben Abdullah F (2010) Exogenous proline effects on photosynthetic performance and antioxidant defense system of young olive tree. J Agric Food Chem 58:4216–4222

Bennett M, Gallagher M, Fagg J, Bestwick C, Paul T, Beale M, Mansfield J (1996) The hypersensitive reaction, membrane damage, and accumulation of autofluorescent phenolics in lettuce cells challenged by *Bremia lactucae*. Plant J 9:851–865

Bradford MM (1976) A rapid and sensitive method for the quantitation of microgram quantities of protein utilizing the principle of protein–dye binding. Anal Biochem 72:248–254

Buchter R, Stromberg A, Schmelzer E, Kombrink E (1997) Primary structure and expression of acidic (class II) chitinase in potato. Plant Mol Biol 35:749–761

Cabrefiga J, Montesinos E (2005) Analysis of aggressiveness of *Erwinia amylovora* using disease-dose and time relationships. Phytopathology 95:1430–1437

Caten CE, Jinks JL (1968) Spontaneous variability of single isolates of *Phytophthora infestans*. Can J Bot 46:329–348

Chapman EJ, Carrington JC (2007) Specialization and evolution of endogenous small RNA pathways. Nat Rev Genet 8:884–896

Cho M, Moinuddin SGA, Helms GL, Hishiyama S, Eichinger D, Davin LB, Lewis ND (2003) (+)-Larreatricin hydroxylase, an enantio-specific polyphenol oxidase from the creosote bush (*Larrea tridentata*). Proc Natl Acad Sci USA 100:10641–10646

Dicke M, Baldwin IT (2010) The evolutionary context for herbivore-induced plant volatiles: beyond the 'cry for help'. Trends Plant Sci 15:167–175

Dixon RA, Achnine L, Kota P, Liu CJ, Reddy MS, Wang L (2002) The phenylpropanoid pathway and plant defence—a genomics perspective. Mol Plant Pathol 3:371–390

Do PT, Prudent M, Sulpice R, Causse M, Fernie AR (2010) The influence of fruit load on the tomato pericarp metabolome in a *Solanum chmielewskii* introgression line population. Plant Physiol 154:1128–1142

Fernie AR, Roscher A, Ratcliffe RG, Kruger NJ (2001) Fructose 2,6-bisphosphate activates pyrophosphate: fructose-6-phosphate 1-phosphotransferase and increases triose phosphate to hexose phosphate cycling in heterotrophic cells. Planta 212:250–263

Ferrer JL, Austin MB, Stewart C Jr, Noel JP (2008) Structure and function of enzymes involved in the biosynthesis of phenylpropanoids. Plant Phys Biochem 46:356–370

Fry W (2008) *Phytophthora infestans*: the plant (and *R* gene) destroyer. Mol Plant Pathol 9:385–402

Gachomo EW, Seufferheld MJ, Kotchoni SO (2010) Melanization of appressoria is critical for the pathogenicity of *Diplocarpon rosae*. Mol Biol Rep 37:3583–3591

Haas BJ et al (2009) Genome sequence and analysis of the Irish potato famine pathogen *Phytophthora infestans*. Nature 461:393–398

Hakimi SM, Krohn BM, Stark DM (2006) Monsanto Technology LLC. Method of imparting disease resistance to plants by reducing polyphenol oxidase activities. United States Patent US 7,122,719 B2

Halim VA, Eschen-Lippold L, Altmann S, Birschwilks M, Scheel D, Rosahl S (2007) Salicylic acid is important for basal defense of *Solanum tuberosum* against *Phytophthora infestans*. Mol Plant Microbe Interact 20:1346–1352

Hemaiswarya S, Soudaminikkutty R, Narasumani ML, Doble M (2011) Phenylpropanoids inhibit protofilament formation of *Escherichia coli* cell division protein FtsZ. J Med Microbiol 60:1317–1325

Hernandez-Romero D, Solano F, Sanchez-Amat A (2005) Polyphenol oxidase activity expression in *Ralstonia solanacearum*. Appl Environ Microbiol 71:6808–6815

Hoegen E, Stromberg A, Pihlgren U, Kombrink E (2002) Primary structure and tissue-specific expression of the pathogenesis-related protein PR-1b in potatodagger. Mol Plant Pathol 3:329–345

Huckelhoven R (2007) Cell wall-associated mechanisms of disease resistance and susceptibility. Annu Rev Phytopathol 45:101–127

Jacobson ES (2000) Pathogenic roles for fungal melanins. Clin Microbiol Rev 13:708–717

Judelson HS, Tooley PW (2000) Enhanced polymerase chain reaction methods for detecting and quantifying *Phytophthora infestans* in plants. Phytopathology 90:1112–1119

Judelson HS, Tani S, Narayan RD (2009) Metabolic adaptation of *Phytophthora infestans* during growth on leaves, tubers and artificial media. Mol Plant Pathol 10:843–855

Kroner A, Hamelin G, Andrivon D, Val F (2011) Quantitative resistance of potato to *Pectobacterium atrosepticum* and *Phytophthora infestans*: integrating PAMP-triggered response and pathogen growth. PLOS ONE 6:e23331

La Camera S, Gouzerh G, Dhondt S, Hoffmann L, Fritig B, Legrand M, Heitz T (2004) Metabolic reprogramming in plant innate immunity: the contributions of phenylpropanoid and oxylipin pathways. Immunol Rev 198:267–284

Leiss KA, Maltese F, Choi YH, Verpoorte R, Klinkhamer PG (2009) Identification of chlorogenic acid as a resistance factor for thrips in chrysanthemum. Plant Physiol 150:1567–1575

Li L, Steffens JC (2002) Overexpression of polyphenol oxidase in transgenic tomato plants results in enhanced bacterial disease resistance. Planta 215:239–247

Liu Q, Paroo Z (2010) Biochemical principles of small RNA pathways. Annu Rev Biochem 79:295–319

Llorente B, Bravo-Almonacid F, Cvitanich C, Orlowska E, Torres HN, Flawia MM, Alonso GD (2010) A quantitative real-time PCR method for *in planta* monitoring of *Phytophthora infestans* growth. Lett Appl Microbiol 51:603–610

Llorente B et al (2011) Safety assessment of nonbrowning potatoes: opening the discussion about the relevance of substantial equivalence on next generation biotech crops. Plant Biotechnol J 9:136–150

Lou Z, Wang H, Zhu S, Ma C, Wang Z (2011) Antibacterial activity and mechanism of action of chlorogenic acid. J Food Sci 76:M398–M403

Lyr H (1962) Detoxification of heartwood toxins and chlorophenols by higher fungi. Nature 195:289–290

Maher EA, Bate NJ, Ni W, Elkind Y, Dixon RA, Lamb CJ (1994) Increased disease susceptibility of transgenic tobacco plants with suppressed levels of preformed phenylpropanoid products. Proc Natl Acad Sci USA 91:7802–7806

Martinez E, Duvnjak Z (2006) Enzymatic degradation of chlorogenic acid using a polyphenol oxidase preparation from the white-rot fungus *Trametes versicolor* ATCC 42530. Process Biochem 41:1835–1841

Mayer AM (2006) Polyphenol oxidases in plants and fungi: going places? A review. Phytochemistry 67:2318–2331

McCurdy RD, McGrath JJ, Mackay-Sim A (2008) Validation of the comparative quantification method of real-time PCR analysis and a cautionary tale of housekeeping gene selection. Gene Ther Mol Biol 12:15–24

Montesano M, Hyytiainen H, Wettstein R, Palva ET (2003) A novel potato defence-related alcohol:$NADP^+$ oxidoreductase induced in response to *Erwinia carotovora*. Plant Mol Biol 52:177–189

Montesano M, Brader G, Ponce de Leon I, Palva ET (2005) Multiple defence signals induced by *Erwinia carotovora* ssp. *carotovora* elicitors in potato. Mol Plant Pathol 6:541–549

Nakayama T et al (2000) Aureusidin synthase: a polyphenol oxidase homolog responsible for flower coloration. Science 290:1163–1166

Nicot N, Hausman JF, Hoffmann L, Evers D (2005) Housekeeping gene selection for real-time RT-PCR normalization in potato during biotic and abiotic stress. J Exp Bot 56:2907–2914

Niggeweg R, Michael AJ, Martin C (2004) Engineering plants with increased levels of the antioxidant chlorogenic acid. Nat Biotechnol 22:746–754

Nikitina VE, Vetchinkina EP, Ponomareva EG, Gogoleva YV (2010) Phenol oxidase activity in bacteria of the genus *Azospirillum*. Microbiology 79:327–333

Nowara D et al (2010) HIGS: host-induced gene silencing in the obligate biotrophic fungal pathogen *Blumeria graminis*. Plant Cell 22:3130–3141

Orlowska E, Fiil A, Kirk HG, Llorente B, Cvitanich C (2012) Differential gene induction in resistant and susceptible potato cultivars at early stages of infection by *Phytophthora infestans*. Plant Cell Rep 31:187–203

Ozcelik B, Kartal M, Orhan I (2011) Cytotoxicity, antiviral and antimicrobial activities of alkaloids, flavonoids, and phenolic acids. Pharm Biol 49:396–402

Payne G, Parks TD, Burkhart W, Dincher S, Ahl P, Metraux JP, Ryals J (1988) Isolation of the genomic clone for pathogenesis-related protein-1a from *Nicotiana tabacum* cv Xanthi-Nc. Plant Mol Biol 11:89–94

Payyavula RS, Navarre DA, Kuhl JC, Pantoja A, Pillai SS (2012) Differential effects of environment on potato phenylpropanoid and carotenoid expression. BMC Plant Biol 12:39

Payyavula RS, Navarre DA, Kuhl J, Pantoja A (2013) Developmental effects on phenolic, flavonol, anthocyanin, and carotenoid metabolites and gene expression in potatoes. J Agric Food Chem 61:7357–7365

Pinero S, Rivera J, Romero D, Cevallos MA, Martinez A, Bolivar F, Gosset G (2007) Tyrosinase from *Rhizobium etli* is involved in nodulation efficiency and symbiosis-associated stress resistance. J Mol Microbiol Biotechnol 13:35–44

Richter C, Dirks ME, Gronover CS, Prüfer D, Moerschbacher BM (2012) Silencing and heterologous expression of *ppo-2* indicate a specific function of a single polyphenol oxidase isoform in resistance of dandelion (*Taraxacum officinale*) against *Pseudomonas syringae* pv. tomato. Mol Plant Microbe Interact 25:200–210

Rivero RM, Ruiz JM, Garcia PC, Lopez-Lefebre LR, Sanchez E, Romero L (2001) Resistance to cold and heat stress:

accumulation of phenolic compounds in tomato and watermelon plants. Plant Sci 160:315–321

Rommens CM, Ye J, Richael C, Swords K (2006) Improving potato storage and processing characteristics through all-native DNA transformation. J Agric Food Chem 54:9882–9887

Shadle GL, Wesley SV, Korth KL, Chen F, Lamb C, Dixon RA (2003) Phenylpropanoid compounds and disease resistance in transgenic tobacco with altered expression of L-phenylalanine ammonia-lyase. Phytochemistry 64:153–161

Si-Ammour A, Mauch-Mani B, Mauch F (2003) Quantification of induced resistance against *Phytophthora* species expressing GFP as a vital marker: beta-aminobutyric acid but not BTH protects potato and *Arabidopsis* from infection. Mol Plant Pathol 4:237–248

Simon P (2003) Q-gene: processing quantitative real-time RT-PCR data. Bioinformatics 19:1439–1440

Steiner U, Oerke EC (2007) Localized melanization of appressoria is required for pathogenicity of *Venturia inaequalis*. Phytopathology 97:1222–1230

Steiner U, Schliemann W, Böhm H, Strack D (1999) Tyrosinase involved in betalain biosynthesis of higher plants. Planta 208:114–124

Sung WS, Lee DG (2010) Antifungal action of chlorogenic acid against pathogenic fungi, mediated by membrane disruption. Pure Appl Chem 82:219–226

Thipyapong P, Hunt MD, Steffens JC (2004a) Antisense downregulation of polyphenol oxidase results in enhanced disease susceptibility. Planta 220:105–117

Thipyapong P, Melkonian J, Wolfe DW, Steffens JC (2004b) Suppression of polyphenol oxidases increases stress tolerance in tomato. Plant Sci 167:693–703

Thygesen PW, Dry IB, Robinson SP (1995) Polyphenol oxidase in potato. A multigene family that exhibits differential expression patterns. Plant Physiol 109:525–531

VanEtten HD, Mansfield JW, Bailey JA, Farmer EE (1994) Two classes of plant antibiotics: phytoalexins versus "Phytoanticipins". Plant Cell 6:1191–1192

Villarino M, Sandín-España P, Melgarejo P, De Cal A (2011) High chlorogenic and neochlorogenic acid levels in immature peaches reduce *Monilinia laxa* infection by interfering with fungal melanin biosynthesis. J Agric Food Chem 59:3205–3213

Vogt T (2010) Phenylpropanoid biosynthesis. Mol Plant 3:2–20

Whisson SC, Avrova AO, Van West P, Jones JT (2005) A method for double-stranded RNA-mediated transient gene silencing in *Phytophthora infestans*. Mol Plant Pathol 6:153–163

Yang HY, Chen CW (2009) Extracellular and intracellular polyphenol oxidases cause opposite effects on sensitivity of *Streptomyces* to phenolics: a case of double-edged sword. PLOS ONE 4:e7462

Yao K, De Luca V, Brisson N (1995) Creation of a metabolic sink for tryptophan alters the phenylpropanoid pathway and the susceptibility of potato to *Phytophthora infestans*. Plant Cell 7:1787–1799

Yu D, Liu Y, Fan B, Klessig DF, Chen Z (1997) Is the high basal level of salicylic acid important for disease resistance in potato? Plant Physiol 115:343–349